

## UC Merced

### UC Merced Previously Published Works

**Title**

Speed dependence of friction on single-layer and bulk MoS<sub>2</sub> measured by atomic force microscopy

**Permalink**

<https://escholarship.org/uc/item/2b8107zw>

**Journal**

Applied Physics Letters, 116(7)

**ISSN**

0003-6951

**Authors**

Acikgoz, Ogulcan  
Baykara, Mehmet Z

**Publication Date**

2020-02-18

**DOI**



10.1063/1.5142712

Peer reviewed

# Speed dependence of friction on single-layer and bulk MoS<sub>2</sub> measured by atomic force microscopy

Cite as: Appl. Phys. Lett. **116**, 071603 (2020); <https://doi.org/10.1063/1.5142712>

Submitted: 16 December 2019 . Accepted: 07 February 2020 . Published Online: 19 February 2020

Ogulcan Acikgoz , and Mehmet Z. Baykara 



View Online



Export Citation




CrossMark



## Measure Ready M91 FastHall™ Controller

A revolutionary new instrument  
for complete Hall analysis

See the video 

 Lake Shore  
CRYOTRONICS

# Speed dependence of friction on single-layer and bulk MoS<sub>2</sub> measured by atomic force microscopy

Cite as: Appl. Phys. Lett. **116**, 071603 (2020); doi: [10.1063/1.5142712](https://doi.org/10.1063/1.5142712)

Submitted: 16 December 2019 · Accepted: 7 February 2020 ·

Published Online: 19 February 2020



View Online



Export Citation



CrossMark

Ogulcan Acikgoz  and Mehmet Z. Baykara 

## AFFILIATIONS

Department of Mechanical Engineering, University of California Merced, Merced, California 95343, USA

<sup>a)</sup> Author to whom correspondence should be addressed: [mehmet.baykara@ucmerced.edu](mailto:mehmet.baykara@ucmerced.edu)

## ABSTRACT

We perform atomic force microscopy (AFM) experiments on mechanically exfoliated, single-layer and bulk molybdenum disulfide (MoS<sub>2</sub>) in order to probe friction forces as a function of sliding speed. The results of the experiments demonstrate that (i) friction forces increase logarithmically with respect to sliding speed, (ii) there is no correlation between the speed dependence of friction and the number of layers of MoS<sub>2</sub>, and (iii) changes in the speed dependence of friction can be attributed to changes in the physical characteristics of the AFM probe, manifesting in the form of varying contact stiffness and tip-sample interaction potential parameters in the thermally activated Prandtl-Tomlinson model. Our study contributes to the formation of a mechanistic understanding of the speed dependence of nanoscale friction on two-dimensional materials.

Published under license by AIP Publishing. <https://doi.org/10.1063/1.5142712>

Two-dimensional (2D) materials, including but not limited to graphene, have been the subject of intense research over the past decade and a half.<sup>1–3</sup> While the majority of such work has centered on their unusual electronic properties and the related implications for devices, the mechanical characteristics of 2D materials, such as their elastic deformation<sup>4</sup> and failure mechanisms,<sup>5</sup> are also of immense interest.<sup>6</sup> A third area of inquiry in terms of mechanical properties of 2D materials involves their tribology. Specifically, the potential use of 2D materials as solid lubricants in micro- and nano-scale mechanical systems draws significant attention, mainly due to the fact that liquid-based lubrication schemes are not easily applicable on such small length scales.<sup>7–9</sup> Consequently, friction on 2D materials was evaluated in a number of studies conducted primarily via atomic force microscopy (AFM), focusing on the effects of applied load, the number of layers, structural defects, and humidity, among others.<sup>10–17</sup>

Despite the extensive amount of work performed toward elucidating friction mechanisms on 2D materials, very few results were published on the dependence of friction forces on sliding speed.<sup>18</sup> This is potentially a critical concern, as components in various micro- and nano-scale mechanical systems designed to be lubricated by 2D materials are expected to move in a wide range of speeds during operation. As such, a potential degradation of lubricative character at certain sliding speeds could result in unexpected device failure and consequently necessitate new approaches in component design.

Aside from the practical concerns described above, the general question of whether or how friction depends on sliding speed is a subject of ongoing research. Coulomb's experiments, performed in the 18th century, have led to the conclusion that friction does *not* depend on sliding speed, which is considered to be one of the "classical" laws of friction.<sup>19</sup> On the other hand, the use of AFM in friction research revealed a variety of speed dependencies for friction on the nanoscale, with certain studies pointing to a logarithmic increase in friction with sliding speed<sup>20–23</sup> while others have found no dependence<sup>24</sup> and even decreasing friction with increasing speed based on variations in interface chemistry<sup>25</sup> or normal load.<sup>26</sup>

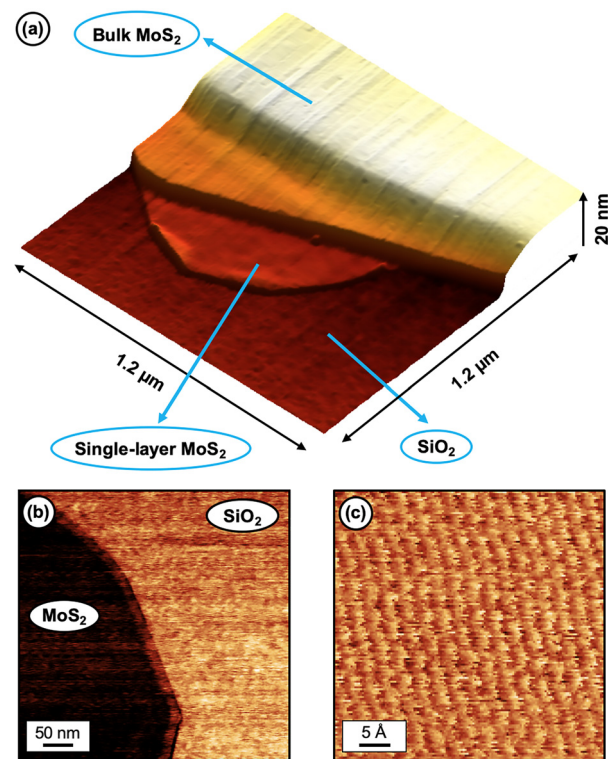
Here, we utilize AFM to investigate the speed dependence of friction on mechanically exfoliated, single-layer and bulk samples of MoS<sub>2</sub>. The motivation to focus on MoS<sub>2</sub> stems partially from the fact that, in its bulk form, it is widely employed as a solid lubricant, either by itself or as an additive in liquid lubricants.<sup>27</sup> Additionally, the lubricative properties of MoS<sub>2</sub> improve significantly under vacuum (as opposed to graphite, the bulk form of graphene), making it an attractive solid lubricant for applications including but not limited to spacecraft components.<sup>28</sup> Consequently, single- and few-layer MoS<sub>2</sub> have the potential to be an effective solid lubricant for micro- and nano-scale mechanical systems designed for operation under low-humidity or vacuum conditions.

The experiments reported here were performed under ordinary laboratory conditions using a commercial AFM instrument (Asylum

Research, Cypher VRS). MoS<sub>2</sub> flakes were prepared by the mechanical exfoliation of a bulk MoS<sub>2</sub> crystal onto SiO<sub>2</sub> substrates.<sup>29</sup> The measurements were conducted using two types of silicon cantilevers (MikroMasch HQ:CSC38 and Bruker RESPA-20), with normal spring constant values (0.05 N/m and 0.36 N/m, respectively) determined by the Sader method.<sup>30</sup> The cantilevers were calibrated for lateral force measurements using the method proposed by Ogletree *et al.*<sup>31</sup> During the measurements, no normal load was applied to the cantilevers; as such, the effective normal load was solely due to adhesion. AFM measurements were performed in contact-mode, whereby the lateral force signal was collected together with topography maps. The measurements focused on areas of a few nanometer-square on single-layer and bulk regions of a single MoS<sub>2</sub> flake, at scanning speeds ( $v$ ) ranging from 2.9 nm/s to 1560 nm/s. All lateral force maps collected in these experiments showed atomic-scale *stick-slip* character. In order to minimize the potential effect of gradual tip changes with varying time on the acquired data, the scanning speed was varied randomly.<sup>22</sup> The mean friction force corresponding to a particular measurement was determined from *friction loops* constructed from the forward and backward lateral force maps.<sup>32</sup> Four consecutive scans were performed at each scanning speed to increase statistical significance; the friction force reported for each speed ( $F_L$ ) reflects the mean and standard deviation of these four measurements. The effective lateral stiffness at the tip-sample junction ( $k_{\text{eff}}$ ) was experimentally determined from lateral force maps, by studying the slopes during the “stick” phase.<sup>20</sup> No significant change in  $k_{\text{eff}}$  values was observed with respect to scanning speed, in accordance with previous results.<sup>18</sup>

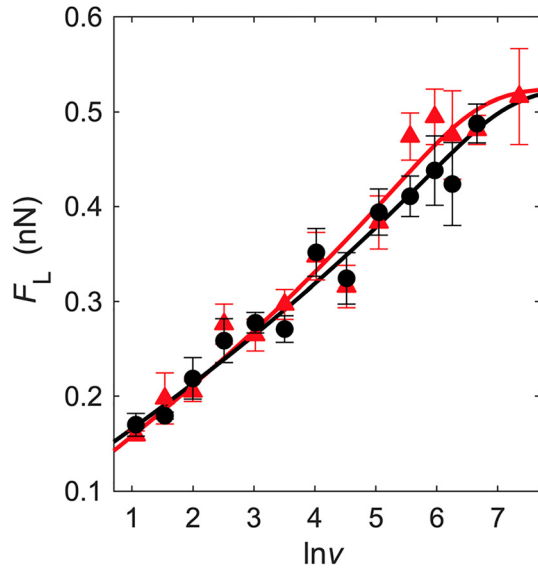
Figure 1(a) shows a three-dimensional representation of a topographical AFM image, which comprises the multi-layer MoS<sub>2</sub> flake on which the experiments were performed and the SiO<sub>2</sub> substrate on which the flake was deposited. The shallowest part of the flake is about  $\sim 1.0$  nm higher than the underlying SiO<sub>2</sub> substrate; the highest part of the flake is at a height of  $\sim 20$  nm and can thus be considered “bulk.” Despite the fact that the value of  $\sim 1.0$  nm is somewhat larger than what was reported for single-layer MoS<sub>2</sub> flakes in some studies ( $\sim 0.8$  nm),<sup>33</sup> the fact that it is significantly less than the minimum height for bi-layer MoS<sub>2</sub> ( $\sim 1.3$  nm) establishes that this region of the flake is indeed single-layer. While the large-scale friction force map in Fig. 1(b) demonstrates the remarkable solid lubrication effect that is achieved on SiO<sub>2</sub> by single-layer MoS<sub>2</sub>, the friction force map in Fig. 1(c) exemplifies the atomic-scale stick-slip character that is observed in smaller scans, from which the speed dependence data presented in the following parts of this Letter have been extracted.

Figure 2 shows the friction force that was recorded as a function of scanning speed, by means of consecutive measurements on single-layer and bulk MoS<sub>2</sub> samples performed with the same cantilever (RESPA-20), over the course of a single day. The results demonstrate that friction force increases logarithmically with sliding speed on both types of samples. Remarkably, the dependence of the experimentally acquired friction data on speed is very similar for both single-layer and bulk MoS<sub>2</sub>, in contrast to results published recently for graphene.<sup>18</sup> The logarithmic increase in friction with sliding speed can be understood by means of the thermally activated Prandtl–Tomlinson (PTT) model.<sup>21,34</sup> In the classic Prandtl–Tomlinson model,<sup>35,36</sup> a point mass (that represents the tip apex in AFM) is attached to a base (that represents the cantilever’s fixed base in AFM) by means of an elastic spring (which represents the *effective* lateral stiffness of the



**FIG. 1.** (a) Three-dimensional representation of a topographical AFM image showing the multi-layer MoS<sub>2</sub> flake on which the experiments were performed and the SiO<sub>2</sub> substrate on which the flake was deposited. (b) Large-scale friction force map recorded on an area that includes the single-layer region of the MoS<sub>2</sub> flake and the SiO<sub>2</sub> substrate, demonstrating the lubricating effect of MoS<sub>2</sub> (bright: high friction; dark: low friction). The mean friction force recorded on MoS<sub>2</sub> is  $\sim 2.5$  times smaller than the one recorded on SiO<sub>2</sub>. (c) Small-scale friction force map recorded on single-layer MoS<sub>2</sub>, showing atomic-scale stick-slip.

sample-tip-cantilever system), whereby the base and consequently the point mass are moved laterally over a one-dimensional, periodic potential energy landscape that arises due to energy interactions between the tip apex and the sample surface. During this motion, the tip apex periodically gets *stuck* in the minima of the energy landscape. Due to fact that the base keeps moving with constant speed over the sample surface, the model spring that connects the tip apex to the cantilever gets stretched with passing time, until the elastic energy stored in the spring is sufficient to overcome the potential energy barrier around the well, at which point the tip apex *slips* to the next potential minimum, with the energy stored in the spring being dissipated through phononic mechanisms. The repeated process of being stuck in and then slipping out of potential energy wells gives rise to the atomic-scale *stick-slip* character of lateral force maps such as the one shown in Fig. 1(c). The  $F_L$  value recorded in the AFM experiments simply reflects the force experienced by the spring in the Prandtl–Tomlinson model. This relatively simple picture becomes slightly more complex when the effect of a non-zero temperature is considered. At a given temperature, the thermal energy associated with the tip apex facilitates its ability to slip to adjacent potential minima in the direction of motion, by effectively lowering



**FIG. 2.** Friction force as a function of the logarithm of the sliding speed (in units of nm/s) for single-layer (black circles) and bulk (red triangles) MoS<sub>2</sub> samples, demonstrating very similar dependencies of friction force on sliding speed. The solid lines are fits by the PTT model.

the associated energy barrier. This also allows the formation of a basic understanding of the effect of sliding speed on friction: With increasing sliding speed, the number of attempts for thermally activated jumps in a given potential well decreases. This leads to a monotonic increase in  $F_L$  until a limiting value (i.e., a plateau) is reached at high speeds, representing the scenario when the base is moving so fast that thermally activated jumps can no longer lower the friction. Analytically, the overall picture is captured by the following equation:<sup>21</sup>

$$\frac{1}{\beta k_B T} (F^* - F_L)^{3/2} = \ln \frac{v_0}{v} - \frac{1}{2} \ln \left( 1 - \frac{F_L}{F^*} \right), \quad (1)$$

where  $\beta$  is a parameter that depends on the shape of the tip-sample interaction potential,  $k_B$  is the Boltzmann constant,  $F^*$  is the “limiting value” of the friction force expected at temperature  $T = 0$  K or at sufficiently high sliding speeds,  $v$  is the sliding speed, and  $v_0$  is a characteristic speed that depends on parameters  $\beta$ ,  $F^*$ , and  $k_{\text{eff}}$ , as well as the “attempt frequency” of the tip apex relevant for jumps to adjacent potential minima ( $f_0$ ), in the following fashion:

$$v_0 = \frac{2f_0 \beta k_B T}{3k_{\text{eff}} \sqrt{F^*}}. \quad (2)$$

In order to analyze the speed dependence results presented in Fig. 2 for single-layer and bulk MoS<sub>2</sub> in more detail, Eqs. (1) and (2) were utilized to fit the experimental data (solid lines in Fig. 2), with  $F^*$ ,  $\beta$ , and  $f_0$  as free parameters. The obtained results for the parameters are reported in Table I, where the experimentally recorded values for  $k_{\text{eff}}$  are also listed. As one can already see in Fig. 2, the fits performed according to Eqs. (1) and (2) closely follow the experimental data, with very similar rates of increase in friction with sliding speed. This qualitative observation is reproduced by the similarity in obtained fit

**TABLE I.** Parameters ( $F^*$ ,  $\beta$ , and  $f_0$ ) extracted from the fits of the data presented in Fig. 2 via Eqs. (1) and (2) and experimentally obtained effective lateral stiffness values ( $k_{\text{eff}}$ ) for measurements on single-layer and bulk MoS<sub>2</sub>.

	$F^*$ (nN)	$\beta$ ( $\times 10^6$ ) (N <sup>3/2</sup> /J)	$f_0$ (kHz)	$k_{\text{eff}}$ (N/m)
Single-layer	$0.53 \pm 0.01$	$0.34 \pm 0.02$	$13.9 \pm 2.5$	$2.01 \pm 0.79$
Bulk	$0.53 \pm 0.01$	$0.39 \pm 0.03$	$7.8 \pm 1.5$	$2.02 \pm 0.80$

parameters, in particular by  $\beta$  and  $F^*$ . The close similarity in the obtained results suggests that the number of layers has no discernible effect on how friction depends on sliding speed for MoS<sub>2</sub>, meaning that the key characteristics of the tip-sample interaction potential (embodied by  $\beta$  and  $F^*$ ) do not significantly change with the increasing number of MoS<sub>2</sub> layers. On the other hand, it needs to be considered that the specifics of the tip-sample interaction depend also on the atomic-scale physical characteristics of the tip apex itself. In particular, changes in the atomic structure of the tip apex can change the specifics of the interaction potential, e.g., by changing the depth of potential minima and/or the overall shape of the potential profile. Consequently, similar results obtained for  $\beta$  and  $F^*$  on single-layer and bulk MoS<sub>2</sub> suggest that the atomic-scale characteristics of the tip apex were very similar for both sets of experiments, i.e., that there was no substantial tip change during the course of the measurements. This idea is further corroborated by observing that the  $k_{\text{eff}}$  values are nearly identical for both single-layer and bulk MoS<sub>2</sub>. Finally, the latter finding implies that the in-plane stiffness of an MoS<sub>2</sub> layer (which plays a major role in determining  $k_{\text{eff}}$ ) does not depend on the existence or absence of additional layers under it, which can be understood by considering the weak, van der Waals nature of the interaction between individual MoS<sub>2</sub> layers.

To complement the results reported above, additional experiments were performed on single-layer MoS<sub>2</sub>. In particular, friction on a particular area on the single-layer region was repeatedly measured as a function of sliding speed, in the form of three separate experimental runs performed over the course of two days with the same cantilever (HQ:CSC38). The results of the experiments, reported in Fig. 3, are in striking contrast to Fig. 2: The speed dependence of friction is significantly different for the three runs, with a clear increase in the rate with which friction increases with sliding speed. This observation is quantitatively captured by the fit parameters  $\beta$  and  $F^*$  that are reported in Table II. In particular,  $\beta$  and  $F^*$  values significantly increase with each experimental run, to nearly four and three times their original values, respectively. Considering that all runs were performed on the same area of the same single-layer MoS<sub>2</sub> flake, the reported results lead to the conclusion that atomic-scale changes in the tip apex must have led to the observed differences in the speed dependence of friction. In particular, the increase in  $F^*$  could imply the formation of a larger (i.e., blunter) tip apex over time, resulting in a larger total friction force.<sup>22</sup> A study of the experimentally obtained lateral stiffness values at the tip-sample junction ( $k_{\text{eff}}$ ) corroborates this conclusion: With the increasing number of runs, the tip-sample junction becomes stiffer, pointing to atomic-scale changes in the tip apex, which result in laterally stiffer structures. While it is conceivable that this trend could saturate in a stable tip structure after a certain number of runs, substantial



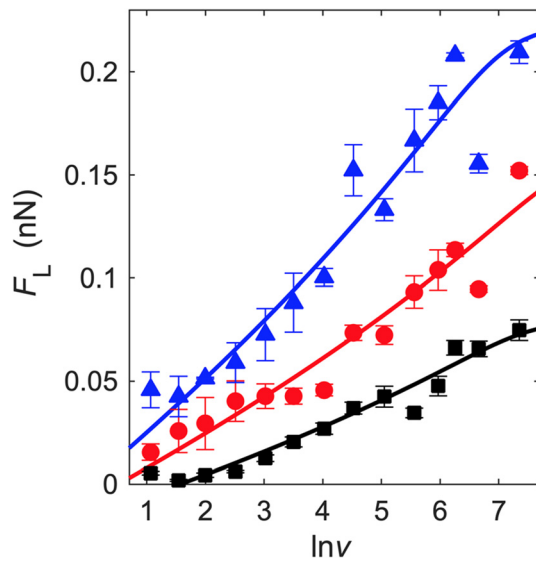


**FIG. 3.** Friction force as a function of the logarithm of the sliding speed (in units of nm/s) for three consecutive runs (Run 1: black squares, Run 2: red circles, and Run 3: blue triangles) performed on a particular area of the single-layer MoS<sub>2</sub> sample, demonstrating increasingly stronger dependencies of friction force on sliding speed. The solid lines are fits by the PTT model.

tip changes that lead to a loss of atomic-scale stick-slip prevented such a study from being conducted.

A particular aspect of the analysis that has so far not been discussed is the fact that the obtained values for the attempt frequency  $f_0$  reported in Tables I and II do not necessarily follow the trends observed for the other tip-sample-interaction-specific parameters  $\beta$ ,  $F^*$ , and  $k_{\text{eff}}$ . While  $f_0$  values in our study are on the same order of magnitude as those reported in certain previous studies,<sup>21</sup> it was also shown that  $f_0$  is sensitive to the extent of the instrumental noise present during the measurements and how well it couples to the tip-sample junction.<sup>22,37</sup> As such, the differences in  $f_0$  in our measurements can be potentially ascribed to changes in instrumental noise. Finally, it needs to be mentioned that the lack of a plateau region in our experiments (with the potential exception of the bulk measurement in Fig. 2 and Run 3 in Fig. 3) prevents an independent verification of the fit parameter  $F^*$ , with the implication that there can be other combinations of parameters that could fit the experiments similarly well. This, however, does not change the main conclusions drawn earlier: (i) the rate with which friction increases with sliding speed on MoS<sub>2</sub> does not seem to depend on the number of layers and (ii) tip

**TABLE II.** Parameters ( $F^*$ ,  $\beta$ , and  $f_0$ ) extracted from the fits of the data presented in Fig. 3 via Eqs. (1) and (2) and experimentally obtained effective lateral stiffness values ( $k_{\text{eff}}$ ) for three measurement runs on single-layer MoS<sub>2</sub>.

	$F^*$ (nN)	$\beta$ ( $\times 10^6$ ) ( $\text{N}^{3/2}/\text{J}$ )	$f_0$ (kHz)	$k_{\text{eff}}$ (N/m)
Run I	$0.079 \pm 0.002$	$0.037 \pm 0.003$	$20.2 \pm 5.3$	$0.45 \pm 0.10$
Run II	$0.160 \pm 0.002$	$0.078 \pm 0.007$	$28.9 \pm 9.6$	$0.52 \pm 0.09$
Run III	$0.223 \pm 0.002$	$0.139 \pm 0.014$	$7.2 \pm 2.0$	$0.58 \pm 0.08$

apex changes can significantly affect the speed dependence of friction on MoS<sub>2</sub>.

In this Letter, we studied the speed dependence of friction on single-layer and bulk MoS<sub>2</sub> by means of atomic-scale, stick-slip lateral force maps acquired via AFM. Our results revealed a logarithmic dependence of friction on sliding speed, in accordance with the PTT model. It was found that the number of layers has no discernible effect on how friction scales with speed on MoS<sub>2</sub>. Moreover, changes in the atomic structure of the tip apex—manifesting in the form of variations in tip-sample-interaction-specific parameters of the PTT model and the effective lateral stiffness at the tip-sample junction—were found to significantly affect the speed dependence of friction. The approach employed here can be extended to other 2D materials, where utmost care has to be exercised to analyze and, if possible, exclude the effect of tip apex changes on the acquired data.

This work was supported by the Merced Nanomaterials Center for Energy and Sensing (MACES) via the National Aeronautics and Space Administration (NASA) under Grant No. NNX15AQ01.

## REFERENCES

- <sup>1</sup>K. S. Novoselov, V. I. Fal'ko, L. Colombo, P. R. Gellert, M. G. Schwab, and K. Kim, *Nature* **490**, 192 (2012).
- <sup>2</sup>S. Das, J. A. Robinson, M. Dubey, H. Terrones, and M. Terrones, *Annu. Rev. Mater. Res.* **45**, 1 (2015).
- <sup>3</sup>X. Li and H. W. Zhu, *J. Materomics* **1**, 33 (2015).
- <sup>4</sup>C. Lee, X. Wei, J. W. Kysar, and J. Hone, *Science* **321**, 385 (2008).
- <sup>5</sup>P. Zhang, L. Ma, F. Fan, Z. Zang, C. Peng, P. E. Loya, Z. Liu, Y. Gong, J. Zhang, X. Zhang *et al.*, *Nat. Commun.* **5**, 3782 (2014).
- <sup>6</sup>D. Akinwande, C. J. Brennan, J. S. Bunch, P. Egberts, J. R. Felts, H. Gao, R. Huang, J.-S. Kim, T. Li, Y. Li *et al.*, *Extrem. Mech. Lett.* **13**, 42 (2017).
- <sup>7</sup>K.-S. Kim, H.-J. Lee, C. Lee, S.-K. Lee, H. Jang, J.-H. Ahn, J.-H. Kim, and H.-J. Lee, *ACS Nano* **5**, 5107 (2011).
- <sup>8</sup>D. Berman, A. Erdemir, and A. V. Sumant, *Mater. Today* **17**, 31 (2014).
- <sup>9</sup>D. Berman, A. Erdemir, and A. V. Sumant, *ACS Nano* **12**, 2122 (2018).
- <sup>10</sup>C. Lee, Q. Li, W. Kalb, X. Z. Liu, H. Berger, R. W. Carpick, and J. Hone, *Science* **328**, 76 (2010).
- <sup>11</sup>P. Egberts, G. H. Han, X. Z. Liu, A. T. C. Johnson, and R. W. Carpick, *ACS Nano* **8**, 5010 (2014).
- <sup>12</sup>T. Demirbaş and M. Z. Baykara, *J. Mater. Res.* **31**, 1914 (2016).
- <sup>13</sup>Z. J. Ye, A. Balkanci, A. Martini, and M. Z. Baykara, *Phys. Rev. B* **96**, 115401 (2017).
- <sup>14</sup>M. Tripathi, F. Awaja, R. A. Bizao, S. Signetti, E. Iacob, G. Paolicelli, S. Valeri, A. Dalton, and N. M. Pugno, *ACS Appl. Mater. Interfaces* **10**, 44614 (2018).
- <sup>15</sup>F. Lavini, A. Calò, Y. Gao, E. Alibetti, T.-D. Li, T. Cao, G. Li, L. Cao, C. Aruta, and E. Riedo, *Nanoscale* **10**, 8304 (2018).
- <sup>16</sup>M. R. Vazirisereshk, H. Ye, Z. Ye, A. Otero-de-la-Roza, M.-Q. Zhao, Z. Gao, A. T. C. Johnson, E. R. Johnson, R. W. Carpick, and A. Martini, *Nano Lett.* **19**, 5496 (2019).
- <sup>17</sup>A. Schumacher, N. Kruse, R. Prins, E. Meyer, R. Lüthi, L. Howald, H.-J. Güntherodt, and L. Scandella, *J. Vac. Sci. Technol., B* **14**, 1264 (1996).
- <sup>18</sup>F. Ptak, C. M. Almeida, and R. Prioli, *Sci. Rep.* **9**, 14555 (2019).
- <sup>19</sup>B. Bhushan, *Introduction to Tribology* (Wiley, New York, 2013).
- <sup>20</sup>E. Gnecco, R. Bennewitz, T. Gyalog, C. Loppacher, M. Bammerlin, E. Meyer, and H.-J. Güntherodt, *Phys. Rev. Lett.* **84**, 1172 (2000).
- <sup>21</sup>E. Riedo, E. Gnecco, R. Bennewitz, E. Meyer, and H. Brune, *Phys. Rev. Lett.* **91**, 084502 (2003).
- <sup>22</sup>X. Z. Liu, Z. Ye, Y. Dong, P. Egberts, R. W. Carpick, and A. Martini, *Phys. Rev. Lett.* **114**, 146102 (2015).
- <sup>23</sup>L. Jansen, H. Holscher, H. Fuchs, and A. Schirmeisen, *Phys. Rev. Lett.* **104**, 256101 (2010).
- <sup>24</sup>O. Zworner, H. Holscher, U. D. Schwarz, and R. Wiesendanger, *Appl. Phys. A* **66**, S263 (1998).

- <sup>25</sup>J. Chen, I. Ratera, J. Y. Park, and M. Salmeron, *Phys. Rev. Lett.* **96**, 236102 (2006).
- <sup>26</sup>W. G. Ouyang, S. N. Ramakrishna, A. Rossi, M. Urbakh, N. D. Spencer, and A. Arcifa, *Phys. Rev. Lett.* **123**, 116102 (2019).
- <sup>27</sup>M. R. Vazirisereshk, A. Martini, D. A. Strubbe, and M. Z. Baykara, *Lubricants* **7**, 57 (2019).
- <sup>28</sup>A. A. Voevodin and J. S. Zabinski, *Compos. Sci. Technol.* **65**, 741 (2005).
- <sup>29</sup>K. S. Novoselov, A. K. Geim, S. V. Morozov, D. Jiang, Y. Zhang, S. V. Dubonos, I. V. Grigorieva, and A. A. Firsov, *Science* **306**, 666 (2004).
- <sup>30</sup>J. E. Sader, J. W. M. Chon, and P. Mulvaney, *Rev. Sci. Instrum.* **70**, 3967 (1999).
- <sup>31</sup>D. F. Ogletree, R. W. Carpick, and M. Salmeron, *Rev. Sci. Instrum.* **67**, 3298 (1996).
- <sup>32</sup>U. D. Schwarz, P. Koster, and R. Wiesendanger, *Rev. Sci. Instrum.* **67**, 2560 (1996).
- <sup>33</sup>H. Li, G. Lu, Z. Yin, Q. He, H. Li, Q. Zhang, and H. Zhang, *Small* **8**, 682 (2012).
- <sup>34</sup>Y. Sang, M. Dube, and M. Grant, *Phys. Rev. Lett.* **87**, 174301 (2001).
- <sup>35</sup>U. D. Schwarz and H. Holscher, *ACS Nano* **10**, 38 (2016).
- <sup>36</sup>O. E. Dagdeviren, *Nanotechnology* **29**, 315704 (2018).
- <sup>37</sup>Y. L. Dong, H. Y. Gao, A. Martini, and P. Egberts, *Phys. Rev. E* **90**, 012125 (2014).